

Magnetic phase diagram of the $U(Ni_{1-x}Cu_x)_2Ge_2$ system studied by ac-susceptibility measurements and neutron diffraction of polycrystalline samples

Moshe Kuznietz, Haim Pinto, Hanania Etedgui, and Mordechai Melamud

Nuclear Research Centre-Negev, P.O. Box 9001, 84 190 Beer-Sheva, Israel

(Received 4 January 1993; revised manuscript received 26 April 1993)

Polycrystalline $U(Ni_{1-x}Cu_x)_2Ge_2$ solid solutions, investigated by ac-susceptibility measurements and neutron diffraction, exhibit the $ThCr_2Si_2$ -type crystallographic structure and magnetic ordering of the uranium sublattice, with moments along the tetragonal axis: antiferromagnetic type-I (AF-I) [$\mathbf{k}=(0,0,1)$] for $x=0, 0.25$, and 0.50 ; ferromagnetic below T_C , becoming at $T_0 (< T_C)$: AF-I, ferrimagnetic [$\mathbf{k}=(0,0,2/3)$], and AF-IA [$\mathbf{k}=(0,0,1/2)$] for $x=0.75, 0.90$, and 0.95 , respectively; and ferromagnetic for $x=1$. The magnetic phase diagram (temperature versus composition) of the $U(Ni_{1-x}Cu_x)_2Ge_2$ system is proposed, and is discussed in relation to the variation in the number of conduction electrons (via Ruderman-Kittel-Kasuya-Yosida-type interactions).

I. INTRODUCTION

We have lately been engaged in the study of the magnetic ordering in UM_2Ge_2 compounds and $U(M,M')_2Ge_2$ solid solutions ($M, M'=Co, Ni, Cu$) by neutron diffraction, supported by ac-susceptibility measurements.¹⁻⁴ We have already studied the compound UCo_2Ge_2 ,^{1,2} the system $U(Co,Cu)_2Ge_2$,³ and the solid solutions $UNiCuGe_2$ and $UCoNiGe_2$.⁴ All materials investigated ($UCoNiGe_2$ excepted⁴) show the common tetragonal crystallographic structure of the $ThCr_2Si_2$ type, with space group $I4/mmm (D_{4h}^{17})$ and two formula units per unit cell.

UNi_2Ge_2 , studied by neutron diffraction, was reported⁵ to order below $T_N=80$ K in the antiferromagnetic type-I structure (AF-I) with a wave vector $\mathbf{k}=(0,0,1)$ and magnetic moments along the tetragonal axis. Magnetization, electrical resistivity, and dc-susceptibility studies⁶ confirmed recently the antiferromagnetic ordering of UNi_2Ge_2 , but with $T_N=77$ K. Three sets of lattice parameters a and c were published⁵⁻⁸ for this compound, which are within 0.2% of each other (or of ours).

UCu_2Ge_2 , studied by neutron diffraction, was reported^{5,9} to order ferromagnetically below $T_C=100$ K, transforming at $T_0=25-40$ K into an antiferromagnetic phase (AF-IA) with a wave vector $\mathbf{k}=(0,0,0.5)$ and magnetic moments along the tetragonal axis. The transition at T_0 was observed once more in high-field magnetization,¹⁰ but not in zero-field electrical resistivity measurements.¹⁰ The ferromagnetic transition was observed at $T_C=107$ K in our ac-susceptibility and neutron-diffraction study.³ However, the transition at T_0 , requiring the appearance of superlattice lines, was not observed in our zero-field neutron-diffraction study.³ Four sets of lattice parameters a and c were published⁶⁻⁹ for this compound, which are within 0.4% of each other (or of ours).

$UNiCuGe_2$, studied by us using neutron diffraction,⁴ was found to order antiferromagnetically below $T_N=140$ K with the AF-I structure.

We extend here our previous studies of UCu_2Ge_2 (Ref.

3) and $UNiCuGe_2$ (Ref. 4) to the $U(Ni_{1-x}Cu_x)_2Ge_2$ system of solid solutions, formed between the compounds UNi_2Ge_2 and UCu_2Ge_2 . Adding the results on UNi_2Ge_2 and the solid solutions with $x=0.25, 0.75$, and 0.90 , a preliminary magnetic phase diagram of the $U(Ni_{1-x}Cu_x)_2Ge_2$ system was presented at the ICM '91 conference.¹¹ We have since studied an additional solid solution in this system, namely, $U(Ni_{0.05}Cu_{0.95})_2Ge_2$, and present here a more complete version of the magnetic phase diagram. An extended report on the $U(Ni_{1-x}Cu_x)_2Ge_2$ system, including detailed experimental results, is published elsewhere.¹²

II. EXPERIMENTAL DETAILS

Polycrystalline samples of the $U(Ni_{1-x}Cu_x)_2Ge_2$ solid solutions with $x=0, 0.25, 0.50, 0.75, 0.90, 0.95$, and 1 were prepared by arc melting of stoichiometric amounts of the constituents in an argon atmosphere. The obtained buttons were annealed at $750^\circ C$ in vacuum for 120 h. Following the annealing, the buttons were crushed into fine powders and examined by x-ray diffraction at room temperature (295 K) to determine the crystallographic structure and lattice parameters at this temperature.

ac-susceptibility measurements, in the 80–295-K temperature range, were done on polycrystalline samples (weighing 280–766 mg; see Table II) of all $U(Ni_{1-x}Cu_x)_2Ge_2$ solid solutions prepared. The ac magnetic field was rather weak (< 10 Oe). Calibration of the ac-susceptibility values was done with a 300-mg polycrystalline sample of Gd_2O_3 for which the χ_M value at 293 K is 51×10^{-3} emu/mol (with $\Theta = -15$ K and $\mu_{eff} = 7.9\mu_B$). These measurements determined the temperatures and types of the magnetic transitions in near-zero magnetic fields, as well as the paramagnetic properties of these materials.

Neutron- ($\lambda=2.4 \text{ \AA}$) diffraction measurements were done with the KANDI-III and US1 diffractometers at the IRR-2 reactor, using 20-g samples in cylindrical aluminum containers. The measurements were per-

formed in a DISPLEX (brand name of a closed-cycle helium cooler made by Air Products Inc.) at room temperature (RT) $T=295$ K and at low temperatures (LT) down to 10 K. These measurements determined the RT and LT crystallographic structure and the LT magnetic structure of the $\text{U}(\text{Ni}_{1-x}\text{Cu}_x)_2\text{Ge}_2$ solid solutions.

III. RESULTS

A. Crystallography

All $\text{U}(\text{Ni}_{1-x}\text{Cu}_x)_2\text{Ge}_2$ solid solutions prepared exhibit a major ThCr_2Si_2 -type phase and minority impurity phases, most noticeable (2%) in UCu_2Ge_2 .

The RT lattice parameters (a, c), as determined by x-ray and neutron diffraction, and the RT fitted position parameter (z) of the germanium atom, as determined by neutron diffraction, of the $\text{U}(\text{Ni}_{1-x}\text{Cu}_x)_2\text{Ge}_2$ solid solutions are given in Table I. The previously published lattice parameters of the compounds UNi_2Ge_2 (Refs. 5–8) and UCu_2Ge_2 (Refs. 5–9) differ by less than 0.4% from the lattice parameters determined in the present study.

The variation of the lattice parameters with x is plotted in Fig. 1. The lattice parameter a drops between $x=0$ and 0.25 and then remains constant (≈ 4.05 Å). The lattice parameter c increases with x rapidly from $x=0$ to 0.25 and then moderately up to $x=1$.

The LT fitted position parameter (z) of the germanium atom falls within the experimental error range of the respective RT value.

B. ac susceptibility

The temperature dependence of the molar ac susceptibility of the solid solutions $\text{U}(\text{Ni}_{1-x}\text{Cu}_x)_2\text{Ge}_2$ in the 80–295-K range is shown in Fig. 2. No susceptibility peak is obtained in this temperature range for UNi_2Ge_2 ($x=0$), in agreement with the neutron-diffraction observation of ordering at $T_N=80\pm 5$ K. One susceptibility peak, corresponding to single magnetic transition, is observed for $x=0.25, 0.50$, and 1. Two susceptibility peaks, corresponding to two consecutive magnetic transitions, are observed for $x=0.75, 0.90$, and 0.95; the lower transition in the latter is almost overshadowed by the higher sharp peak, corresponding to a ferromagnetic

TABLE I. Room-temperature (RT) lattice parameters (a, c) and fitted position parameter (z) of the germanium atom in the $\text{U}(\text{Ni}_{1-x}\text{Cu}_x)_2\text{Ge}_2$ solid solutions. The RT residuals R are from neutron diffraction.

Compound or solid solution	RT lattice parameters			R (%) at RT
	a (Å) (± 0.010)	c (Å) (± 0.020)	z (± 0.001)	
UNi_2Ge_2 ($x=0$)	4.106	9.464	0.384	8.3
$\text{U}(\text{Ni}_{0.75}\text{Cu}_{0.25})_2\text{Ge}_2$	4.054	9.810	0.373	6.3
$\text{U}(\text{Ni}_{0.5}\text{Cu}_{0.5})_2\text{Ge}_2$	4.055	9.970	0.377	2.5
$\text{U}(\text{Ni}_{0.25}\text{Cu}_{0.75})_2\text{Ge}_2$	4.060	10.070	0.376	4.3
$\text{U}(\text{Ni}_{0.1}\text{Cu}_{0.9})_2\text{Ge}_2$	4.060	10.150	0.379	3.5
$\text{U}(\text{Ni}_{0.05}\text{Cu}_{0.95})_2\text{Ge}_2$	4.053	10.190	0.379	2.3
UCu_2Ge_2 ($x=1$)	4.050	10.250	0.379	6.4

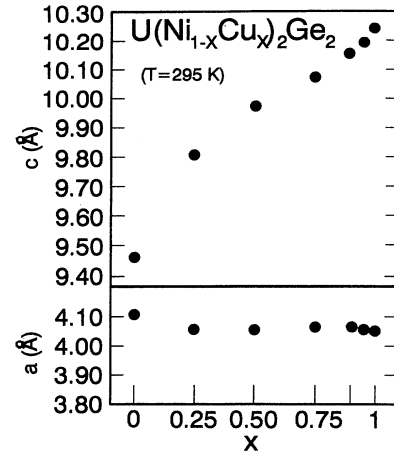


FIG. 1. Variation of the room-temperature lattice parameters (a, c) with the copper content (x) in the $\text{U}(\text{Ni}_{1-x}\text{Cu}_x)_2\text{Ge}_2$ solid solutions (see Table I).

transition. The transition temperatures in the solid solutions are generally higher than those for the end compounds UNi_2Ge_2 and UCu_2Ge_2 and are in good agreement with those obtained by neutron diffraction (see Sec. III C).

The values of the molar susceptibility χ_M measured for the solid solutions $\text{U}(\text{Ni}_{1-x}\text{Cu}_x)_2\text{Ge}_2$ at RT and at the ordering and other transition temperatures (Fig. 2) are given in Table II. The RT values are in the range $(2.9-5.4)\times 10^{-3}$ emu/mol, characteristic of the

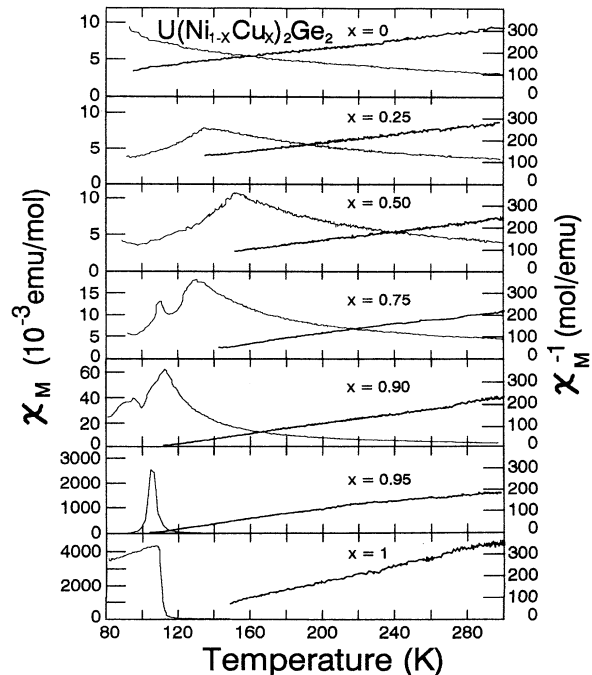


FIG. 2. Temperature dependence of the molar ac susceptibility at 80–295 K (thin curve) and its inverse in the paramagnetic state (thick curve) in polycrystalline samples of the $\text{U}(\text{Ni}_{1-x}\text{Cu}_x)_2\text{Ge}_2$ solid solutions.

TABLE II. ac-susceptibility results in the $U(Ni_{1-x}Cu_x)_2Ge_2$ system: molar susceptibility (χ_M) at room and transition temperatures, effective paramagnetic moment (μ_{eff}), paramagnetic Curie temperature (Θ), and transition temperatures (T_N or T_C, T_0).

x	Sample weight (mg)	χ_M (10^{-3} emu/mol $\pm 4\%$)			μ_{eff} (± 0.2) (μ_B)	Θ (K)	T_C (± 5) (K)	T_N (± 5) (K)	T_0 (± 5) (K)
		at RT	at T_C or T_N	at T_0					
0	766	3.3			3.0	-40 ± 10		80	
0.25	418	3.7	7.8		3.0	-12 ± 12		135	
0.50	331	4.2	10.9		2.8	$+57 \pm 7$		140	
0.75	480	4.4	18.1	13.1	2.7	$+80 \pm 10$	133		117
0.90	619	4.6	61	40	2.7	$+95 \pm 5$	115		95
0.95	450	5.4	2600	68	2.5	$+85 \pm 25$	110		94
1	280	2.9	4300		2.1	$+102 \pm 2$	107		

paramagnetic state. As the temperature is lowered and the ordered state is approached, the value of χ_M increases by a factor of 2–3 for the antiferromagnetic solid solutions ($x=0.25$ and 0.50). This factor rises to 4, 13, and 470 for the solid solutions with $x=0.75$, 0.90 , and 0.95 , which order ferromagnetically and undergo additional transitions to antiferromagnetic or ferrimagnetic phases at lower temperatures T_0 , where this factor is only 3, 9, and 14, respectively. The factor increases to 1500 for the compound UCu_2Ge_2 ($x=1$), which orders ferromagnetically.

Also shown in Fig. 2 is the inverse susceptibility of the solid solutions $U(Ni_{1-x}Cu_x)_2Ge_2$ in the paramagnetic state. The paramagnetic Curie temperature Θ and the effective paramagnetic moment μ_{eff} are obtained [in μ_B (Bohr magnetons)] from the linear part of the inverse susceptibility via the relation

$$(\chi_M)^{-1} = (2.83/\mu_{\text{eff}})^2(T - \Theta), \quad (1)$$

where χ_M is given in emu/mol and $(T - \Theta)$ is given in kelvin. A full linear behavior is observed only for UCu_2Ge_2 , leading to a paramagnetic Curie temperature $\Theta = +102 \pm 2$ K, close to T_C , that is indicative of the ferromagnetic order observed by neutron diffraction. In the other solid solutions, the inverse-susceptibility curves are not linear over the entire temperature range, and so we use the linear parts of the curves at temperatures above 200 K. The values of Θ , obtained from the intersection of these linear parts of the curves with the temperature axis, are listed in Table II.

For UNi_2Ge_2 the value is negative, $\Theta = -40 \pm 10$ K, and is slightly higher than the values reported in Ref. 5 (-54 K) and in Ref. 6 (-71 K). The paramagnetic Curie temperature increases monotonically with x . It is much lower than the ordering temperature in the solid solutions with $x=0$, 0.25 , and 0.50 , indicating antiferromagnetic ordering. It approaches the ordering temperature in the intermediate solid solutions with $x=0.75$, 0.90 , and 0.95 . For UCu_2Ge_2 our value of Θ is similar to the value reported in Ref. 5 ($+100$ K) and is very close to the Curie temperature.

With the molar susceptibilities at RT and the respective values of Θ , the values of μ_{eff} are obtained using Eq. (1). They are all listed in Table II. For UNi_2Ge_2 the value of $\mu_{\text{eff}} = (3.0 \pm 0.2)\mu_B$ is similar to the values report-

ed in Ref. 5 ($3.16\mu_B$) and in Ref. 6 ($3.08\mu_B$). μ_{eff} is nearly constant at $(3.0-2.7)\mu_B$ for the solid solutions with $x \leq 0.95$ and drops to $(2.1 \pm 0.2)\mu_B$ in UCu_2Ge_2 , where its value is different from the values reported in Ref. 5 ($2.40\mu_B$) and in Ref. 10 ($2.65\mu_B$).

C. Magnetic structures determined by neutron diffraction

For all $U(Ni_{1-x}Cu_x)_2Ge_2$ samples investigated, the reflections observed from the RT diffractograms ($h+k+l=\text{even}$) are consistent with the $ThCr_2Si_2$ -type crystallographic structure and the $I4/mmm$ space group. The RT diffractograms show clear variation with x of the relative intensities of the first nuclear reflections ($\{002\}$ and $\{110\}$ with respect to $\{011\}$), as expected from the variation of b , the weighted average scattering length, of the M site ($=Ni_{1-x}Cu_x$), affecting only reflections with $h+k=\text{even}$. The RT residuals (R) are included in Table I. The LT residuals are given with the LT results in Table III.

The LT diffractograms of UNi_2Ge_2 and of all the $U(Ni_{1-x}Cu_x)_2Ge_2$ solid solutions investigated (with $x=0.25$, 0.50 , 0.75 , 0.90 , and 0.95) show magnetic reflections, in addition to the nuclear reflections in the RT diffractograms. In UCu_2Ge_2 the LT diffractogram does not show additional reflections besides the nuclear, but shows magnetic contributions manifested as increased intensities on top of all nuclear reflections except $\{002\}$, as discussed later.

The LT diffractogram of UNi_2Ge_2 (at 10 K) shows additional reflections for which $h+k+l=\text{odd}$ (such as $\{010\}$, $\{012\}$, $\{111\}$), indicating antiferromagnetic ordering of at least the uranium sublattice, with a wave vector $\mathbf{k}=(0,0,1)$ and $+-+-$ stacking of ferromagnetic layers along the tetragonal axis (AF-I). The absence of $\{00l\}$ reflections with odd l indicates that the ordered magnetic moments are along the tetragonal axis. The integrated intensities of the reflections with $h+k+l=\text{odd}$ are in agreement with the ordering of the uranium sublattice, with a fitted ordered magnetic moment of $(1.9 \pm 0.5)\mu_B$. Antiferromagnetism appears at $T_N = 80 \pm 5$ K, and the antiferromagnetic structure is of the same type down to $T = 10$ K.

The LT diffractograms at 10 K of $U(Ni_{0.75}Cu_{0.25})_2Ge_2$

TABLE III. Neutron-diffraction results in the $U(Ni_{1-x}Cu_x)_2Ge_2$ system: ordering temperature (T_N or T_C), transition temperature (T_0), types of ordering, calculated LT residual (R), and uranium ordered magnetic moment at ≈ 10 K (m).

x	T_C (± 5) (K)	T_N (± 5) (K)	Order below T_C or T_N	T_0 (± 5) (K)	Order below T_0	R (%) at 10 K	m (10 K) (μ_B)
0		80	AF-I			8.3	1.9 ± 0.5
0.25		135	AF-I			8.2	2.0 ± 0.4
0.50		140	AF-I			3.4	2.2 ± 0.1
0.75	133		ferro	117	AF-I	5.5	2.2 ± 0.2
0.90	115		ferro	95	ferri	4.3	1.9 ± 0.2
0.95	110		ferro	94	AF-IA	1.6	1.9 ± 0.1
1	107		ferro			7.8	1.9 ± 0.4

($x=0.25$) and of $U(Ni_{0.5}Cu_{0.5})_2Ge_2$ ($x=0.50$) (Ref. 4) are similar to that of UNi_2Ge_2 . These materials are antiferromagnetic, with the AF-I structure as in UNi_2Ge_2 , with T_N increasing to 135 ± 5 and 140 ± 5 K, respectively. The fitted ordered magnetic moments at 10 K are $(2.0 \pm 0.4)\mu_B$ and $(2.2 \pm 0.1)\mu_B$ for $x=0.25$ and 0.50, respectively.

$U(Ni_{0.25}Cu_{0.75})_2Ge_2$ ($x=0.75$) orders ferromagnetically at $T_C=133 \pm 5$ K, as indicated by the ac-susceptibility measurements, showing another transition at $T_0=117 \pm 5$ K to an antiferromagnetic phase. The magnetic structure is again AF-I, as seen from the LT neutron diffractogram (at 10 K) [Fig. 3(a)]. The observed integrated and calculated intensities for the RT and LT neutron-diffraction spectra are listed in Ref. 12. The fitted ordered magnetic moment at 10 K is $(2.2 \pm 0.2)\mu_B$.

$U(Ni_{0.1}Cu_{0.9})_2Ge_2$ ($x=0.90$) orders ferromagnetically at $T_C=115 \pm 5$ K, as indicated by the ac-susceptibility measurements, showing another transition at $T_0=95 \pm 5$ K to a ferrimagnetic phase, characterized by a rather high χ_M at T_0 . The LT neutron diffractogram (at 10 K) [Fig. 3(b)] shows superlattice reflections which can be indexed as $\{hk(l \pm \frac{2}{3})\}$ satellites of the RT nuclear $\{hkl\}$ reflections. The observed integrated and calculated intensities for the RT and LT neutron-diffraction spectra are listed in Ref. 12. The additional reflections correspond to a wave vector $\mathbf{k}=(0,0,\frac{2}{3})$ and ferrimagnetic $++-$ stacking of ferromagnetic layers along the tetragonal axis. The absence of $\{00(l \pm \frac{2}{3})\}$ reflections indicates that the ordered magnetic moments are along the tetragonal axis. Details of the measurements on this solid solution have been published separately.^{12,13} The same ferrimagnetic structure was found in the LT phase (below 53 K) of the related compound UNi_2Si_2 by neutron diffraction on polycrystalline⁵ and single-crystal¹⁴ samples. The fitted ordered magnetic moment of the present material at 10 K is $(1.9 \pm 0.2)\mu_B$.

$U(Ni_{0.05}Cu_{0.95})_2Ge_2$ ($x=0.95$) orders ferromagnetically at $T_C=110 \pm 5$ K, as indicated by the ac-susceptibility measurements, and is characterized by a rather high peak in χ_M at T_C . It undergoes another transition at $T_0=94 \pm 5$ K to an antiferromagnetic phase. The LT neutron diffractogram (at 10 K) [Fig. 3(c)] shows superlattice reflections which can be indexed as $\{hk(l \pm \frac{1}{2})\}$ satellites of the RT nuclear $\{hkl\}$ reflections. The observed

integrated and calculated intensities for the RT and LT neutron-diffraction spectra are listed in Ref. 12. The additional reflections correspond to a wave vector $\mathbf{k}=(0,0,\frac{1}{2})$ and antiferromagnetic $+- -$ stacking of ferromagnetic layers along the tetragonal axis (AF-IA). The absence of $\{00(l \pm \frac{1}{2})\}$ reflections indicates that the ordered magnetic moments are along the tetragonal axis. The same magnetic structure was reported at low temper-

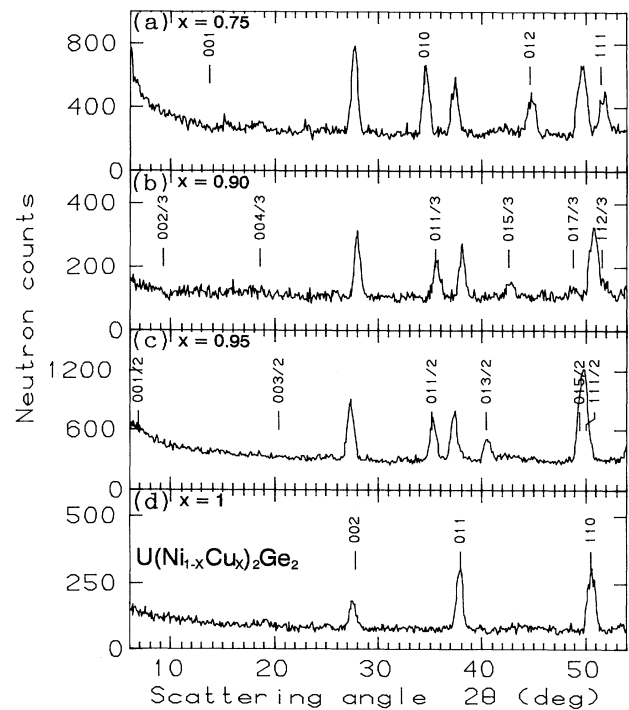


FIG. 3. Neutron- ($\lambda=2.4$ Å) diffraction patterns at 10 K of polycrystalline $U(Ni_{1-x}Cu_x)_2Ge_2$ solid solutions (with the indices of the nuclear reflections omitted): (a) $x=0.75$, showing magnetic reflections and the absence of $\{00l\}$ reflections with odd l ; (b) $x=0.90$, showing satellite magnetic reflections at $\{hk(l \pm \frac{2}{3})\}$ positions around nuclear $\{hkl\}$ positions and the absence of $\{00(l \pm \frac{2}{3})\}$ reflections; (c) $x=0.95$, showing satellite magnetic reflections at $\{hk(l \pm \frac{1}{2})\}$ positions around nuclear $\{hkl\}$ positions and the absence of $\{00(l \pm \frac{1}{2})\}$ reflections; (d) $x=1$ (UCu_2Ge_2), implying magnetic contributions to the nuclear reflections except $\{002\}$.

atures in the previous study of UCu_2Ge_2 (Refs. 5 and 9) and has been reported in the compounds RM_2X_2 [such as $NdFe_2Si_2$ (Ref. 15)]. The fitted ordered magnetic moment of the present material at 10 K is $(1.9 \pm 0.1)\mu_B$.

In the three solid solutions with $x = 0.75, 0.90,$ and 0.95 , the ordered magnetic moments in the ferromagnetic phases (at $T_0 < T < T_C$) are too small to be detected in our neutron-diffraction measurements.

The LT diffractogram (at 10 K) of UCu_2Ge_2 ($x = 1$) [Fig. 3(d)] shows no additional reflections with respect to the RT diffractogram. Additional intensities on all nuclear reflections, except on $\{002\}$, are associated with ferromagnetic ordering of the uranium sublattice along the tetragonal axis. The observed integrated and calculated intensities for the RT and LT neutron-diffraction spectra are listed in Ref. 12. The fitted ordered magnetic moment at 10 K is $(1.9 \pm 0.4)\mu_B$. Ferromagnetism appears at $T_C = 107 \pm 5$ K, and there is no transition to an antiferromagnetic phase down to $T = 10$ K. The same sample has been studied later with the DN2 multidetector at the Siloe reactor in the CEN de Grenoble and found to be ferromagnetic down to 2 K, confirming the above result. The LT AF-IA $(++--)$ phase reported earlier for this compound^{5,9,10} is not observed in our sample, and this is not a problem of resolution, since the same structure is observed in our sample of $U(Ni_{0.05}Cu_{0.95})_2Ge_2$ ($x = 0.95$).

The uranium ordered magnetic moments (at 10 K) as a function of x are given in Table III. The variation of the ordered magnetic moment with temperature in the materials studied is deduced from the temperature variation of the integrated intensity of the first magnetic reflection (depending on the structure): $\{010\}$ for $x = 0, 0.25, 0.50,$ and 0.75 ; $\{01(\frac{1}{3})\}$ for $x = 0.90$; $\{01(\frac{1}{2})\}$ for $x = 0.95$; and $\{011\}$ for $x = 1$.

D. Magnetic phase diagram

The neutron-diffraction results in the $U(Ni_{1-x}Cu_x)_2Ge_2$ system are summarized in Table III. Based on these results, the proposed magnetic phase diagram (temperature versus composition) of the $U(Ni_{1-x}Cu_x)_2Ge_2$ solid solutions, at zero applied magnetic field, is shown in Fig. 4. An antiferromagnetic-ferromagnetic transition occurs for $U(Ni_{0.25}Cu_{0.75})_2Ge_2$ at 117 K, a ferrimagnetic-ferromagnetic transition occurs for $U(Ni_{0.1}Cu_{0.9})_2Ge_2$ at 95 K, and another antiferromagnetic-ferromagnetic transition occurs for $U(Ni_{0.05}Cu_{0.95})_2Ge_2$ at 94 K, as already mentioned above.

IV. DISCUSSION

The neutron-diffraction data determine unambiguously the type of magnetic ordering of the uranium sublattice in the $U(Ni_{1-x}Cu_x)_2Ge_2$ solid solutions. These data are consistent with the ac-susceptibility data, and both characterize the $U(Ni_{1-x}Cu_x)_2Ge_2$ system in a zero applied magnetic field. The direction of the uranium magnetic moments in this system is along the tetragonal axis, independent of magnetic structure type, as found hitherto in all UM_2X_2 compounds and $U(M, M')_2X_2$ solid solutions having the $I4/mmm$ space-group symmetry.

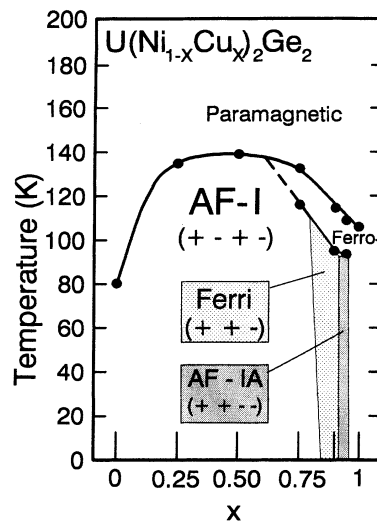


FIG. 4. Proposed magnetic phase diagram (temperature vs composition at zero applied magnetic field) of the $U(Ni_{1-x}Cu_x)_2Ge_2$ system. Most of the diagram is AF-I. Other magnetic structures and magnetic phase transitions are concentrated in the copper-rich side.

An important property is the nonordering of (or rather low magnetic moment on) the (Ni,Cu) sublattices. Nonmagnetic M sublattices are also the common case in the parallel lanthanide compounds LnM_2X_2 .¹⁶ In spite of their nonmagnetic character, the M or (M, M') sublattices determine the type of ordering on the uranium sublattice in the UM_2X_2 and $U(M, M')_2X_2$ systems, respectively, as demonstrated in the present study (Fig. 4). This behavior is basically different from the behavior in systems with other $3d$ transition metals. In the UMn_2X_2 compounds, both manganese and uranium sublattices order magnetically, while in the UFe_2X_2 compounds neither iron or uranium sublattices order magnetically.¹⁷

The common magnetic structure is the AF-I structure, and indeed it covers a wide range of the magnetic phase diagram (temperature versus composition) of the $U(Ni_{1-x}Cu_x)_2Ge_2$ system (Fig. 4). A special peculiarity of this diagram is the ferromagnetic-to-commensurate crossover, which occurs for solid solutions with $x \geq 0.75$ (at 117, 95, and 94 K for $x = 0.75, 0.90,$ and 0.95 , respectively), disappearing close to $x = 1$, where only the ferromagnetic phase exists.

For $x = 0$ (UNi_2Ge_2) our neutron-diffraction results, of AF-I ordering below $T_N = 80$ K, are in agreement with the results of Chelmicki, Leciejewicz, and Zygmunt.⁵ Our uranium ordered magnetic moment (at 10 K) is somewhat lower than theirs ($2.35\mu_B$ at 4.2 K), while our z value at RT is slightly higher than theirs (0.3785).

For $x = 1$ (UCu_2Ge_2) we did not observe the LT ferromagnetic-antiferromagnetic transition, reported by Leciejewicz, Chelmicki, and Zygmunt^{5,9} from their neutron-diffraction results, although our uranium ordered magnetic moment (at 10 K) is close to theirs ($1.61\mu_B$ at 4.2 K) (as are both z values at RT, which are the same, 0.379). A LT transition was also observed by

McAlister, Olivier, and Siegrist¹⁰ in their high-field magnetization results, but not in their zero-field resistivity data. It is not possible that the LT AF-IA phase was overlooked in our experiments. Since the neutron-diffraction resolution of our measurements (at $\lambda=2.4$ Å) is better than the resolution in the measurements of Leciejewicz, Chelmicki, and Zygmunt^{5,9} (at $\lambda=1.326$ Å), we are better set to detect the AF-IA structure, as we have indeed done for the solid solution $U(Ni_{0.05}Cu_{0.95})_2Ge_2$.

It is suggested that the appearance or absence of the AF-IA structure lies in the sample-preparation procedures. The UCu_2Ge_2 sample of Leciejewicz, Chelmicki, and Zygmunt^{5,9} was not annealed, while all our samples, including $U(Ni_{0.05}Cu_{0.95})_2Ge_2$ and UCu_2Ge_2 , were annealed as explained above. The crucial role of annealing in the crystallography and magnetism of the UM_2X_2 compounds has been previously shown for UCo_2Ge_2 .¹⁸ In this case unannealed material has a crystallographic structure of symmetry lower than $I4/mmm$, with a smaller lattice parameter c , and does not order magnetically,^{6,18} while annealed material acquires the $I4/mmm$ space-group symmetry and orders antiferromagnetically at $T_N=175\pm 5$ K.^{1,2,18} As the $U(Ni_{1-x}Cu_x)_2Ge_2$ system in the vicinity of $x=1$ is quite complicated magnetically (see Fig. 4), one can reasonably argue that the appearance of the AF-IA phase in a sample of UCu_2Ge_2 can be due to small deviations from stoichiometry on the copper sublattice. Such deviations, e.g., vacancies in the copper sublattice of the major $ThCr_2Si_2$ -type phase, are accompanied by copper-rich minor phases and are generally removed by annealing. Substoichiometry in the copper sublattice reduces the number of conduction electrons, as does replacement of copper by nickel, both causing the appearance of the AF-IA phase in UCu_2Ge_2 .

The observed changes of the magnetic structure (from Fig. 4) and paramagnetic Curie temperature Θ (from Table II) in the $U(Ni_{1-x}Cu_x)_2Ge_2$ system with the copper content x , as shown in Fig. 5, are the result of the oscillatory dependence on the number of conduction electrons, thereby indicating Ruderman-Kittel-Kasuya-Yosida (RKKY) type behavior. Such a behavior was claimed also in the respective cerium system.¹⁹ RKKY-type interactions are consistent with the observed sensitivity of the magnetic structure to small changes of interatomic distances.

In the $U(Co_{1-z}Cu_z)_2Ge_2$ system both lattice parameters increase with the copper content (z),³ differently

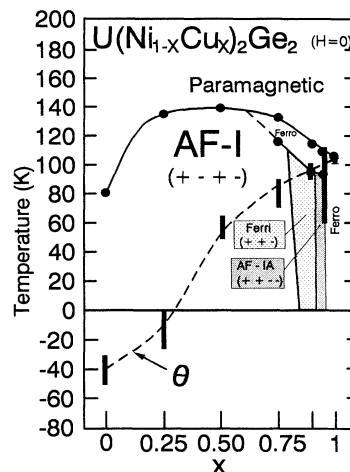


FIG. 5. Variation of the paramagnetic Curie temperature Θ (from Table II) and the magnetic structure (from Fig. 4) with the copper content (x) in the $U(Ni_{1-x}Cu_x)_2Ge_2$ system. The variations are characteristic of a RKKY-type behavior (oscillatory with distance and conduction-electron concentration).

from the variation in the system $U(Ni_{1-x}Cu_x)_2Ge_2$. In the latter a drops slightly and c increases sharply between $x=0$ and 0.25. The unique situation in UNi_2Ge_2 is also evident in similar lanthanide compounds RNi_2X_2 . However, the tetragonal-cell volumes in both $U(Co_{1-z}Cu_z)_2Ge_2$ and $U(Ni_{1-x}Cu_x)_2Ge_2$ systems increase monotonically with the copper content, being similar (159.5 Å³) in UCo_2Ge_2 and UNi_2Ge_2 and 5% higher (168.1 Å³) in UCu_2Ge_2 . Such a variation of tetragonal-cell volume in the UM_2Ge_2 compounds is well correlated with Pearson's metallic radii,²⁰ which for M are 1.252 Å for cobalt, 1.246 Å for nickel, and 1.278 Å for copper. The metallic radius of copper is about 2% higher than the other metallic radii, leading to the increase in the observed tetragonal-cell volume with copper content.

Neutron-diffraction and ac-susceptibility investigations of the parallel system $U(Ni_{1-x}Cu_x)_2Si_2$ (with Si replacing Ge) have already started,²¹ and the determination of the magnetic phase diagram (temperature versus composition) is currently in progress.

ACKNOWLEDGMENT

The authors thank S. Fredo for his skillful help with the preparation of the samples.

¹M. Kuznietz, H. Pinto, H. Etedgui, and M. Melamud, *Phys. Rev. B* **40**, 7328 (1989).

²M. Kuznietz, H. Pinto, and M. Melamud, *J. Magn. Magn. Mater.* **96**, 245 (1991).

³M. Kuznietz, H. Pinto, and M. Melamud, *J. Magn. Magn. Mater.* **83**, 321 (1990).

⁴M. Kuznietz, H. Pinto, and M. Melamud, *J. Appl. Phys.* **67**, 4808 (1990).

⁵L. Chelmicki, J. Leciejewicz, and A. Zygmunt, *J. Phys. Chem. Solids* **46**, 529 (1985).

⁶A. J. Dirkmaat, T. Endstra, E. Knetsch, A. A. Menovsky, G. J. Nieuwenhuys, and J. A. Mydosh, *J. Magn. Magn. Mater.* **84**, 143 (1990).

⁷A. Zygmunt, in *Proceedings of the 2nd International Conference on the Electronic Structure of the Actinides* (Wroclaw, Poland, 1976), edited by J. Mulak, W. Suski, and R. Troc (Zaklad

- Narodowy Imienia Ossolinskich Wydawnictwo Polskiej Akademii Nauk, Wrocław, 1977), pp. 335–341.
- ⁸R. Marazza, R. Ferro, G. Rambaldi, and G. Zanicchi, *J. Less-Common Met.* **53**, 193 (1977).
- ⁹J. Leciejewicz, L. Chelmicki, and A. Zygmunt, *Solid State Commun.* **41**, 167 (1982).
- ¹⁰S. P. McAlister, M. Olivier, and T. Siegrist, *Solid State Commun.* **69**, 113 (1989).
- ¹¹M. Kuznietz, H. Pinto, H. Ettetdgui, and M. Melamud, *Physica B* **180&181**, 55 (1992).
- ¹²M. Kuznietz, H. Pinto, H. Ettetdgui, and M. Melamud, *The Magnetic Phase Diagram of the $U(Ni_{1-x}Cu_x)_2Ge_2$ System Studied by AC-Susceptibility and Neutron Diffraction of Polycrystalline Samples*, NRCN-616 (Nuclear Research Centre–Negev, Beer-Sheva, Israel, 1993).
- ¹³M. Kuznietz, H. Pinto, H. Ettetdgui, and M. Melamud, *Phys. Rev. B* **45**, 7282 (1992).
- ¹⁴H. Lin, L. Rebelsky, M. F. Collins, J. D. Garrett, and W. J. L. Buyers, *Phys. Rev. B* **43**, 13 232 (1991).
- ¹⁵H. Pinto and H. Shaked, *Phys. Rev. B* **7**, 3261 (1973).
- ¹⁶H. Pinto, M. Melamud, M. Kuznietz, and H. Shaked, *Phys. Rev. B* **31**, 508 (1985).
- ¹⁷A. Szytula, S. Siek, J. Leciejewicz, A. Zygmunt, and Z. Ban, *J. Phys. Chem. Solids* **49**, 1113 (1988).
- ¹⁸T. Endstra, G. J. Nieuwenhuys, A. A. Menovsky, and J. A. Mydosh, *J. Appl. Phys.* **69**, 4816 (1991).
- ¹⁹F. Steglich, C. Geibel, S. Horn, U. Ahlheim, M. Lang, G. Sparn, A. Loidl, A. Krimmel, and W. Assmus, *J. Magn. Mater.* **90&91**, 383 (1990).
- ²⁰W. B. Pearson, *The Crystal Chemistry and Physics of Metals and Alloys* (Wiley, New York, 1972).
- ²¹M. Kuznietz, G. André, F. Bourée, H. Pinto, H. Ettetdgui, and M. Melamud, *J. Appl. Phys.* **73**, 6075 (1993).